THE JOURNAL OF PHYSICAL CHEMISTRY B

Article

pubs.acs.org/JPCB

Photophysical Properties and Singlet Oxygen Generation of Three Sets of Halogenated Corroles

Wenli Shao,[†] Hui Wang,*[,†] Shuang He,[‡] Lei Shi,[‡] Kaimei Peng,[‡] Yongfeng Lin,[†] Lei Zhang,*[,†] Liangnian Ji,[†,§] and Haiyang Liu*[,‡]

[†]State Key Laboratory of Optoelectronics Materials and Technologies, Sun-Yat Sen University, Guangzhou 510275, China

[‡]Department of Chemistry, South China University of Technology, Guangzhou 510641, China

[§]School of Chemistry and Chemical Engineering/MOE Laboratory of Bioinorganic and Synthetic Chemistry, Sun-Yat Sen University, Guangzhou 510275, China

S *Supporting Information*

ABSTRACT: The luminescence, excited-state absorption, and singlet oxygen generation measurements were performed on three kinds of halogenated corroles: monohydroxyl halogenated corroles (Corrole-F, Corrole-Cl, Corrole-I), peripherally fluorine-substituted corroles (F0, F5, F10, F15), and gallium complexes (F10-Ga, F15-Ga). The fluorescence intensities progressively decrease whereas the triplet quantum yields, oxygen quenching rates, and singlet oxygen quantum yields increase with the increasing of the monohydroxyl halogen atomic weight. Replacing hydrogen atoms of meso-phenyl groups with fluorine atoms induces the blue-shifts of the emission spectra, higher triplet quantum yield, and smaller oxygen quenching rates. Of all peripherally fluorine-substituted corroles, F10 exhibited the highest singlet oxygen quantum yield. In comparison with the free base corroles, both gallium corrole complexes display much stronger fluorescence with the large blue-shifts of emission peaks and slightly higher triplet quantum yields but smaller oxygen quenching rates and singlet oxygen quantum yields. The reasons for the different photophysical behaviors of these corroles are discussed.

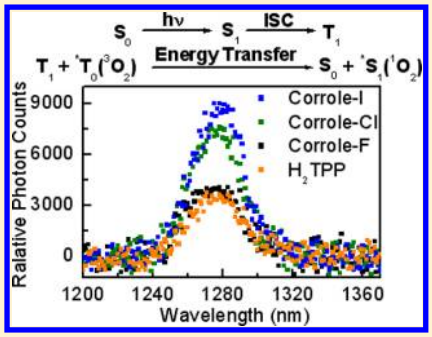

INTRODUCTION

Cancer cell damage based on photodynamic therapy (PDT) lies on the usage of photosensitizers as energy carriers and reaction bridges.[1−3] The generated singlet oxygen ($^1O_2$) is the key cytotoxic agent in PDT.[4−7] A good photosensitizer is demonstrated by its high singlet oxygen quantum yield.[5−8] Promoting intersystem crossing (ISC) process has been considered as an efficient method to improve the singlet oxygen generation.[8,9] Furthermore, long-lived triplet excited states are necessary for singlet oxygen production in general.[8,10] Previous studies have found that the incorporation of heavy atoms in photosensitizer molecules can enhance ISC and is termed as the heavy-atom effect.[5,8,9,11]

Corroles, "the contracted porphyrin analogues",[12] are proving to have unique photochemical and photophysical properties.[13−17] They become a new kind of photosensitizers and have intriguing potential applications in pharmaceuticals,[18,19] photodynamic therapy (PDT),[4,14b] and photodynamic detection (PDD).[20−22] In particular, gallium corrole complexes not only emit intense fluorescence but also are high toxicity in vivo when combined with tumor-targeting cell penetrating proteins, which makes them useful both for tumor detection and elimination.[19,23]

Although the photophysical properties of some corroles have been reported,[9,14,15] the systematical mechanistic study on the heavy-atom effect of substitution and their position on the spectroscopic and photophysical properties is sparse. In particular, the effects of the incorporation of gallium on the photophysical property of corrole have not yet been thoroughly investigated, even though such insight may be very important for exploring the potential applications of the metallocorrole in diagnosis and photodynamic therapy as well as molecular devices. Herein, we present a comparative study of photophysical properties and singlet oxygen production of the family of halogenated corroles and the selected gallium complexes. The investigated corroles are classified as three sets. The first set (Series-1) is monohydroxyl corroles bearing fluorine, chlorine, and iodine atoms on its 10-phenyl group (Corrole-F, Corrole-Cl, Corrole-I). The second set (Series-2) is four peripherally substituted corroles bearing different numbers of fluorine atoms at the meso-phenyl groups (F0, F5, F10, F15). The third set (Series-3) is two fluorinated gallium corrole complexes (F10-Ga, F15-Ga). The steady-state and time-resolved spectroscopic techniques have been used to investigate the influences of heavy-atom effect of halogen atoms, the electronic withdrawing effect of peripherally fluorine atoms as well as the presence of the central metal ion gallium(III) on luminescent properties, excited-state absorption, and singlet

Received: July 10, 2012
Revised: November 11, 2012
Published: November 12, 2012

oxygen generation of these halogenated corroles. The research results are certainly helpful for the design of new PDT or PDD photosentitizers.

EXPERIMENTAL SECTION

Sample Preparation. Series-1[24] and Series-2 corroles[25,26] were synthesized according to the procedures described in the literature. The synthesis of F10-Ga and F15-Ga were prepared from the corresponding free-base corroles, and the procedure is described as follows: a solution of the free-base corroles (0.02 mmol, 17 mg) dissolved in pyridine (15 mL) was added to dry $GaCl_3$ (0.2 mmol, 352.4 mg), and the mixture was heated to reflux under Ar for about 2 h. Then the reaction mixture was evaporated and quickly passed over a chromatography column to remove inorganic salts; purities were obtained after recrystallization from dichloromethane, hexane, and a few drops of pyridine. F10-Ga: ^{1}H NMR ($CDCl_3$, 400 MHz), δ: 9.15 (d, 2H, β-H), 8.84 (m, 4H, β-H), 8.78 (d, 2H, β-H), 8.13 (m, 2H, Ar−H), 7.71 (m, 3H, Ar−H), 6.19 (t, 1H, para-H of pyridine), 5.55 (unresolved t, 2H, meta-H of pyridine), 2.81 (unresolved d, 2H, ortho-H of pyridine). R_f: 0.40. ESI-MS (M^+-pyridine): m/z: 773.1 (calcd 773.2). UV−vis (toluene), λ_{max}/nm ($\varepsilon \times 10^5$ M^{-1} cm^{-1}): 424 (2.52), 575 (0.23), 603 (0.35). F15-Ga: ^{1}H NMR ($CDCl_3$, 400 MHz), δ: 9.13 (d, 2H, β-H), 8.76 (d, 2H, β-H), 8.67 (d, 2H, β-H), 8.63 (d, 2H, β-H), 6.26 (t, 1H, para-H of pyridine), 5.58 (unresolved t, 2H, meta-H of pyridine), 2.81 (unresolved d, 2H, ortho-H of pyridine). ^{19}F-NMR ($CDCl_3$, 400 MHz), δ: −137.82 (d, 6F, ortho-F), −153.85 (m, 3F, para-F), −162.40 (s, 6F, meta-F). R_f: 0.45. ESI-MS (M^+-pyridine): m/z: 863.1 (calcd 863.2). UV−vis (toluene), λ_{max}/nm ($\varepsilon \times 10^5$ M^{-1} cm^{-1}): 423 (2.35), 570 (0.16), 595 (0.20). Figure 1 shows molecular structures of the three sets of corroles. In our experiments, all samples were dissolved in toluene and the concentration is 25 μM. The sample solution was in a 10 mm thick quartz cuvette. Deaerated sample solution was prepared by thaw−freeze−pump cycles eight times and sealed under vacuum.

Measurements. The steady-state absorption and emission spectra of all samples were measured using a PerkinElmer Lambda 850 UV−vis spectrometer and a PerkinElmer LS55 luminescence spectrometer (PE Company), respectively.

The time-resolved fluorescence decays of all samples were measured by using time-resolved fluorescence spectroscopic technology. A Nd:YAG laser (EKSPLA PL2143) and an PG401SH/DFG2 10 ps laser (EKSPLA Co., Lithuania) were employed to generate the excitation pulses with 10 Hz repetition, a full width at half-maximum (fwhm) of 25 ps, and the excitation wavelength of 420 nm. The fluorescence emitted from sample was collected with a set of lenses with big caliber and recorded by a streak camera (Hammatsu C1587) and a CCD (C4742-95) after passing through a monochromator.

The triplet state dynamics of the three sets of corroles were measured using laser flash photolysis apparatus.[27] In this setup, the frequency-doubled output from a pulse Nd:YAG laser (EKSPLA PL2143) with 10 Hz repetition, 25 ps pulse width, and the pulse energy of 5.7 mJ as excitation source. The excitation wavelength is 532 nm. The analyzing light was derived from a 150 W CW xenon lamp. The excitation pulses and analyzing light beam perpendicularly passed through a sample cell. The transient signals, passing through a monochromator (WDG30-Z), were detected by an avalanche photodiode (AD500-8) and amplified by a fast preamplifier

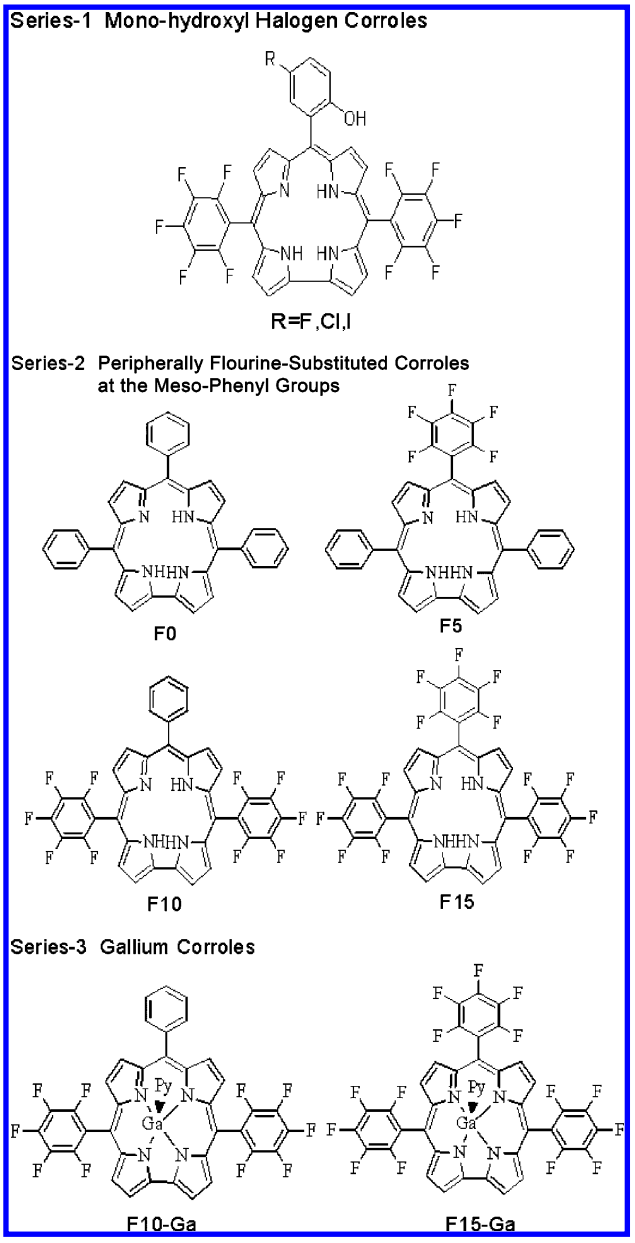

Figure 1. Molecular structures of the three sets of corroles investigated in this study.

with the bandwidth of 350 MHz (SR240A). The amplified signal was recorded on a 300 MHz digital oscilloscope (Tektronix, TDS2024B). The relatively low concentration of the gallium corroles and the free-base corroles with small absorbance of about 0.2 at the excitation wavelength 532 nm can avoid the formation of molecule aggregation.

The steady-state luminescence of singlet oxygen from the three sets of corroles was measured by using a FLS920 spectrofluorimeter (Edinburgh Instruments) with the wavelength range from 600 to 1700 nm. The FLS920 spectrofluorimeter is equipped with a TM300 excitation monochromator and a TM300 emission monochromator equipped with a NIR grating and a Hamamatsu R5509-72 supercooled photomultiplier tube at 193 K. The excitation wavelength is 550 nm.

The relative errors are estimated as 20% on fluorescence quantum yield, 10% for fluorescence lifetime, 23% for triplet

dx.doi.org/10.1021/jp306826p | J. Phys. Chem. B 2012, 116, 14228−14234

lifetime, 10% on triplet quantum yield, and 12% on singlet oxygen quantum yield.

RESULTS AND DISCUSSION

Steady-State Spectra. The steady-state absorption spectra of Series-1, Series-2, and Series-3 corroles in toluene are shown in Figure 2a, 2b, and 2c, respectively. All the examined corroles exibit typical Soret-type bands with the absorption peak around 420 nm and Q-type absorption bands in the region 500−650 nm. The Soret-type absorption of monohydroxyl corrole increases with the increasing of atomic weight of the substituted halogen, which is in agreement with our previous observation.[9] F5 and F15 exhibit the slightly sharper absorption peaks and weaker B-bands absorptions than F0 and F10. As shown in Figure 1c, in comparison with the free-base corroles, two gallium complexes clearly exhibit much stronger absorptions at both Soret and Q bands, accompanied by slightly red-shifts. The steady-state emission spectra of Series-1, Series-2, and Series-3 corroles in toluene after the excitation of 560 nm are also shown in Figure 2a, 2b, and 2c, respectively. The emission peaks and the calculated fluorescence quantum yields of all samples in toluene are summarized in Table 1. As has been already reported,[9] with the increasing of atomic weight of the attached halogen, the fluorescence quantum yield of monohydroxyl halogenated corrole decreases progressively. The emission peaks of all Series-1 corroles are almost at the same wavelength of about 647 nm. The fluorescence spectra of F5, F10, and F15 in Series-2 corroles show the small blue-shifts (≤20 nm) of the fluorescence peaks compared with F0 as shown in Figure 2b, in agreement with the previous report.[14b] The origin may be the decrease of the π-electron density of the corrole ring due to the electron-withdrawing effect of fluorine atoms, which may result in the increase of the energy difference between the HOMO and LUMO.[28,29] No significant trend has been observed for the fluorescence quantum yield in the Series-2 corroles. Previous works have shown that the coordinating solvent and active anion can cause the red-shifts of the emission spectra of gallium corrole.[16,30] In the case reported here, the investigation is focused on the influence of the introduction of gallium on the spectral property of the corroles, which results in about a 40 nm blue-shift of the emission peaks as shown in Figure 2c. The possible reason may be that the introduction of metal ion increases the molecular symmetry and degeneracy of HOMOs and LUMOs,[31] leading to higher energy level of the lowest singlet excited state. Similar metal ion effects have been reported previously in metalloporphyrins.[32,33] Both F10-Ga and F15-Ga show much larger fluorescence quantum yields than those of their corresponding free-base corroles, which may be due to the better planarity of the molecules after the incorporation of gallium into the corrole ring.[34] The results suggest that both position and the intensity of emission peaks are very sensitive to the modification of heavy atoms in the center and peripheral.

Table 1. Summary of Fluorescence Data for the Three Sets of Corroles

compd	emission, λ_{max} [a] (nm)	Φ_{fl} [b]	τ_{fl} [c] (ns)	k_r [d] (10^7 s^{-1})	k_{nr} [e] (10^7 s^{-1})
Corrole-F	647	0.110	4.92	2.24	18.09
Corrole-Cl	647	0.065	4.07	1.67	22.97
Corrole-I	647	0.031	1.94	1.59	49.95
F0	664	0.091	5.07	1.79	17.93
F5	653	0.126	5.64	2.23	15.50
F10	654	0.086	4.52	1.90	20.22
F15	645	0.101	5.15	1.96	17.46
F10-Ga	613, 659	0.245	2.28	10.75	33.11
F15-Ga	603, 657	0.305	2.95	10.34	23.56

[a] λ_{max} stands for the wavelength of two emission bands at the maximum intensity. [b] Fluorescence quantum yields in aerated toluene were calculated based on the fluorescence spectra using H_2TPP (tetraphenylporphyrin) as a standard (Φ_{fl} = 0.11). λ_{ex} = 560 nm. [c] Fluorescence lifetimes in aerated toluene. λ_{ex} = 420 nm. [d] Radiative decay rate constants were determined by using the expression $k_r = \Phi_{fl}/\tau_{fl}$. [e] Nonradiative decay rate constants were obtained from $k_{nr} = (1 - \Phi_{fl})/\tau_{fl}$.

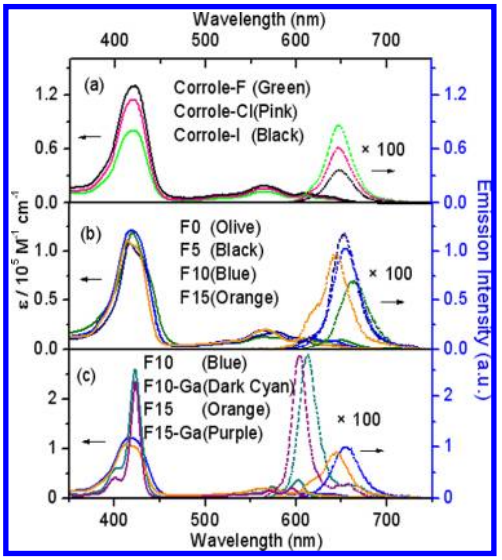

Figure 2. The steady-state absorption (solid lines) and emission (dashed lines) spectra of the three sets of corroles in toluene: (a) monohydroxyl halogen corroles, (b) peripherally fluorine-substituted corroles at the meso-phenyl groups, (c) gallium corroles.

Time-Resolved Fluorescence. The fluorescence decay curves of all corroles at emission peaks after the photo-excitations at 420 nm are displayed in the Supporting Information, which are well fitted with single-exponential functions. The radiative decay rate constants (k_r) and nonradiative decay rate constants (k_{nr}) of all corroles can be determinated from the fluorescence lifetimes (τ_{fl}) and quantum yields,[15] which are summarized in Table 1. In Series-1 corroles, the increase of halogen atomic weight induces the decrease of the fluorescence lifetimes, in agreement with our earlier report.[9] Meanwhile, the k_r decreased and the k_{nr} greatly increased with the increasing of the atomic weight of halogen atoms. In Series-2 corroles, F5 and F15 present slightly longer fluorescence lifetimes and larger values of k_r, however, smaller values of k_{nr} than those of F0 and F10. In the four peripherally substituted corroles, F5 and F10 show the largest values of k_r and k_{nr}, respectively. The fluorescence lifetimes of two gallium complexes are substantially shorter than those of the corresponding free base compounds, due almost to their larger k_r and k_{nr}, which are consistent with previous reports.[16,34]

Triplet-State Transient Absorption Spectra. To further investigate the triplet-state dynamics of the three sets corroles, the experiments of laser flash photolysis have been performed. Figure 3 shows the evolution of the transient absorption spectra of Corrole-I, F10, and F10-Ga selected from Series-1, Series-2,

dx.doi.org/10.1021/jp306826p | J. Phys. Chem. B 2012, 116, 14228−14234

and Series-3 corroles in aerated (a) and deaerated toluene (b) after the photoexcitations at 532 nm. The transient absorption spectra of all samples are similar and dominated by a broad positive absorption bands ranging from about 440 to 540 nm with the maximum at around 460 nm due to the triplet−triplet ($T_1 \rightarrow T_n$) absorption and by the complete negative absorption bands within the range from 540 to 590 nm and smaller than 440 nm, which are assigned to the ground-state bleaching compared with their ground-state absorption spectra shown in Figure 2. The transient absorption spectra of other corroles in both aerated and deaerated toluenes have also been measured and displayed in the Supporting Information. The spectral features are similar to those of Corrole-I, F10, and F10-Ga, which exhibit the strongest triplet state absorptions in Series-1, Series-2, and Series-3 corroles, respectively.

The triplet−triplet molar absorption coefficients ε_T of the three sets of corroles in toluene can be estimated using the singlet depletion method:[35]

$$\varepsilon_T = \varepsilon_S \frac{\Delta OD_T}{\Delta OD_S} \quad (1)$$

where ΔOD_T and ΔOD_S are the transient absorption changes at the maximum of the positive band and the minimum of bleaching band, respectively, and ε_S refers to the ground-state molar absorption coefficient at the minimum of bleaching band. Furthermore, the triplet quantum yields Φ_T and the intersystem crossing rates k_{isc} for all samples can be obtained according to eq 2 (comparative actinometry method)[35,36] and eq 3,[37] respectively.

$$\Phi_T = \Phi_{T(std)} \frac{\Delta OD_T}{\Delta OD_{T(std)}} \frac{\varepsilon_{T(std)}}{\varepsilon_T} \quad (2)$$

$$k_{isc} = \frac{\Phi_T}{\tau_{fl}} \quad (3)$$

The subscript "std" stands for the standard sample. τ_{fl} is the fluorescence lifetime of the tested sample. Here, H_2TPP is as the standard sample ($\Phi_{T(H_2TPP)} = 0.8$, $\varepsilon_T \approx 35\,000$ M^{-1} cm^{-1}).[36] The calculated triplet quantum yields and the intersystem-crossing rates are compiled in Table 2.

The results show that the increasing of the atomic weight of halogen atoms leads to the increase of both the triplet quantum yields Φ_T and intersystem-crossing rates k_{isc}, which can be well explained by the heavy atom effect.[8] Substitution of hydrogen atoms with fluorine atoms in the corrole rings also results in the increases in both Φ_T and k_{isc}, the maxima of which has been observed in F10. The present of the central metal ion gallium(III) slightly increases the Φ_T and k_{isc} of the gallium corrole complexes, which are due primarily to the heavy atom effect.[16] Furthermore, the structure rigidity of gallium corrole complexes can reduce the internal conversion (IC) probability and facilitate the intersystem crossing.[16,34] These results suggest that the heavy atom effect induced by the halogen atoms (Series-1 and Series-2) and metal ion−gallium(III) (Series-3) can enhance the intersystem crossing (ISC) probability via spin−orbital coupling. However, in Series-2 compounds, the change in triplet quantum yields does not follow the trend of the increase of the atomic number of the peripherally fluorine atoms, which may be due to the difference of the position of the fluorine substituents, causing different effects on electron withdrawing in corroles.[28] This suggests that the triplet-state

Table 2. Summary of Triplet State Parameters and Singlet Oxygen Quantum Yields for the Three Sets of Corrole in Toluene

compd	τ_T[a] (ns)	τ_T^0[b] (μs)	k_q^T[c] (10^9 M^{-1} s^{-1})	ε_T[d] (M^{-1} cm^{-1})	k_{isc}[e] (10^8 s^{-1})	Φ_T[f]	Φ_Δ[h]
Corrole-F	256	89	1.855	21 125	1.28	0.63	0.50
Corrole-Cl	238	75	1.990	24 492	2.14	0.87	0.78
Corrole-I	199	63	2.385	25 031	4.69	0.91	0.86
F0	149	28	3.178	16 941	0.71	0.36	0.34
F5	192	75	2.471	22 596	1.21	0.68	0.61
F10	218	91	2.179	31 702	1.62	0.73	0.70
F15	241	104	1.975	30 960	1.24	0.64	0.58
F10-Ga	419	64	1.129	37 779	3.38	0.77	0.57
F15-Ga	502	67	0.941	39 000	2.34	0.69	0.52

[a]The triplet lifetimes in deaerated toluene. [b]The triplet lifetimes in aerated toluene. [c]The oxygen quenching rate constants of triplet state. [d]The triplet state molar extinction coefficients at the maximum absorption. [e]The intersystem-crossing rates. [f]The triplet quantum yields were obtained from eq 2. [h]Singlet oxygen quantum yields were calculated by eq 5.

population is related to not only the heavy atom effect but also the distribution of intramolecular electron cloud.

The insets of Figures 3a and 3b display the triplet-state kinetic traces monitored at 460 nm for Corrole-I, F10, and 450 nm for F10-Ga in aerated and deaerated conditions, respectively. The experimental data are well fitted with a single-exponential function. Under deaerated toluene, the lowest triplet-state lifetimes for all investigated corroles are of the order of microseconds, which are substantially longer than those on the time scale of nanoseconds in aerated condition, where O_2 quenches the triplet states of corroles by analogy to porphyrin.[38] The fitted triplet lifetimes of the three sets of corroles are listed in Table 2. Under both aerated and deaerated conditions, the triplet lifetime of corrole decreases with the increasing of the atomic weight of halogen atom but increases with the increment of the number of the peripherally fluorine atoms. The triplet lifetimes of two gallium corroles become longer in aerated condition but are shorter in deaerated condition compared with the free-base corroles. The shortening of the triplet lifetimes observed in Series-1 and Series-3 corroles under deaerated condition should be due to the enhanced heavy atom effects with the increasing of the atomic weight of halogen atoms or the insertion of gallium.[39] The increase of the triplet lifetimes observed in Series-2 with the increase of the number of the peripherally fluorine atoms may be derived from the continuous decrease of the electronic density in the π-system of the corrole as the capacity of the electron withdrawing increases.[28] According to eq 4 (the Stern−Volmer equation), the oxygen quenching rate constant k_q^T can be calculated:[40]

$$k_q^T = \left[\frac{1}{\tau_T} - \frac{1}{\tau_T^0}\right]\frac{1}{[O_2]} \quad (4)$$

where τ_T and τ_T^0 are the triplet lifetimes under the aerated and deaerated conditions, respectively; $[O_2]$ represents the oxygen concentration, which is 2.1×10^{-3} M in aerated toluene at room temperature.[41] The k_q^T values of all samples are listed in Table 2. The k_q^T values progressively increase with the increasing of atomic weight of the substituted halogen but significantly decrease with the increment of the number of the

dx.doi.org/10.1021/jp306826p | J. Phys. Chem. B 2012, 116, 14228−14234

peripherally fluorine atoms and the insertion of gallium. This indicates that the triplet states of Series-2 and Series-3 compounds are less sensitive to the oxygen with respect to the Series-1 corroles.

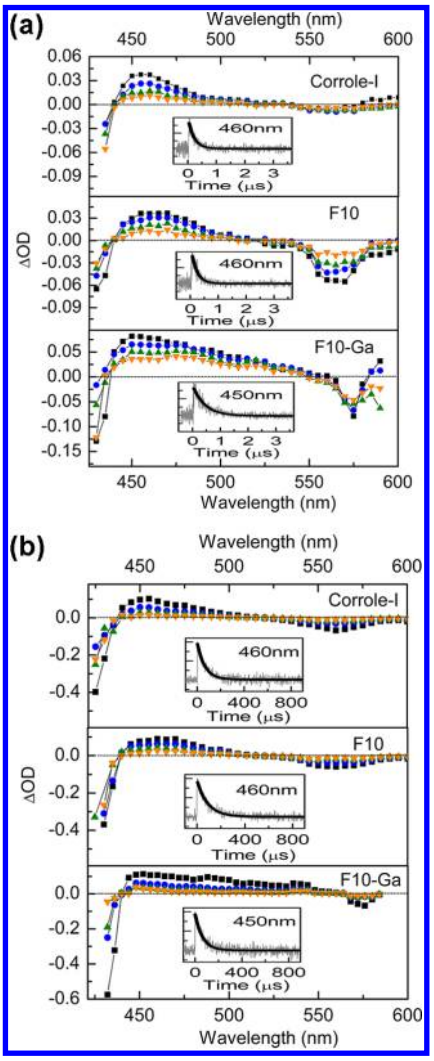

Figure 3. Transient absorption spectra of Corrole-I, F10, and F10-Ga excited at 532 nm: (a) at various delay times 60 ns (black), 120 ns (blue), 200 ns (olive), and 300 ns (orange) in aerated toluene; (b) at various delay times 5 μs (black), 50 μs (blue), 100 μs (olive), and 150 μs (orange) in deaerated toluene. Insets show the kinetic traces monitored at 460 nm for Corrole-I and F10 and 450 nm for F10-Ga.

Singlet Oxygen Generation from the Three Sets of Corroles. Figure 4 displays the steady-state emission spectra of singlet oxygen of Series-1, Series-2 and Series-3 corroles in aerated toluene after the photoexcitation of 550 nm (Q-band absorption). All samples exhibit the emission bands ranging from 1240 to 1320 nm with the peak at about 1270 nm. The singlet oxygen quantum yields Φ_Δ for all samples can be determined by using eq 5 (comparative actinometry method):[35,42]

$$\Phi_\Delta = \Phi_\Delta^{std} \frac{I}{I_{std}} \frac{1 - 10^{-A^{std}}}{1 - 10^{-A}} \quad (5)$$

where Φ_Δ^{std} (0.7)[14b] is the singlet oxygen quantum yield of H_2TPP as the standard sample in aerated toluene, I and I_{std} refer to the singlet oxygen emission intensities at the peaks for the tested sample and H_2TPP, respectively, and A and A^{std} stand for the ground-state absorbance of the tested sample and H_2TPP at the excited wavelength of 550 nm, respectively. The singlet oxygen quantum yields of the three sets of corroles are shown in Table 2.

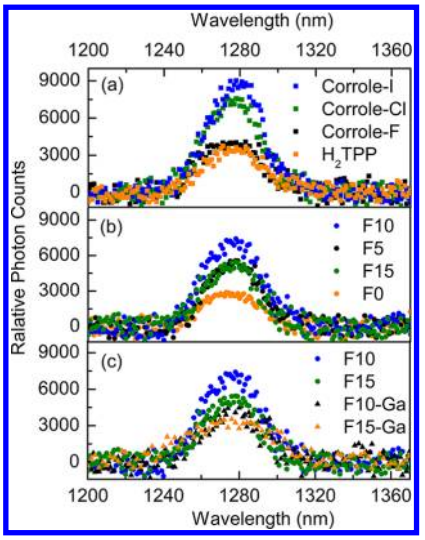

Figure 4. Singlet oxygen luminescene detected in aerated toluene after excitation at 550 nm for optically matched solutions of the three sets of corroles: (a) monohydroxyl halogen corroles, (b) peripherally fluorine-substituted corroles at the meso-phenyl groups, and (c) gallium corroles.

The results show that the increase of the atomic weight of halogen significantly induces the increase in the singlet oxygen quantum yield within the Series-1 corroles. Similarly, fluorine substitution results in the increase in the singlet oxygen quantum yield, the maximum of which was obtained for F10. Contrastingly, the incorporation of gallium slightly reduces the singlet oxygen quantum yield, which may be due to inefficient quenching of the triplet state by oxygen.[40] The experimental data indicate that the effects of substituents and their position on the generation of the singlet oxygen are materially diverse.

First, the singlet oxygen quantum yields follow qualitatively the trends of the triplet quantum yields and intersystem-crossing rates in Series-1 and Series-2 compounds. This reflects that the triplet-state population can directly affect the singlet oxygen quantum yield. On the other hand, the presence of the central metal ion gallium(III) slightly enhances the triplet state population, but the singlet oxygen quantum yields become lower instead. It suggests that the singlet oxygen quantum yields are not completely determined by the triplet quantum yields. It was known that the final step of the singlet oxygen generation process is an energy transfer from triplet photosensitizer to ground state oxygen (triplet oxygen).[39b] Therefore, the efficiency of singlet oxygen generation should depend on not only ISC pathway of a photosentizer but also the efficiency of energy transfer from triplet state of a photosensitizer to ground-state oxygen. Moreover, the energy transfer can occur via the triplet-state quenching of photosensitizer by oxygen.[43] The data in Table 2 demonstrate that the oxygen quenching rate constants of the two gallium complexes are much smaller than those of the corresponding free-base corroles, which may ultimately reduce the efficiency of the energy transfer from

dx.doi.org/10.1021/jp306826p | J. Phys. Chem. B 2012, 116, 14228−14234

excited triple states of the gallium complexes to the ground state of molecule oxygen.

Second, peripherally fluorine-substituted corroles (F5, F10, F15) and gallium complexes (F10-Ga, F15-Ga) exhibit the modest blue-shifts as compared to the F0 and free-base corroles, respectively, as shown in Figure 2. This indicates that the introduction of the peripheral fluorine and the central gallium may give rise to larger energy gap between the lowest excited singlet state and the ground state. Similar behavior should occur between the lowest excited triplet state and the ground state,[44] which may reduce the spectral overlap between the corroles and the oxygen; therefore, the slower energy transfer takes place from the lowest triplet state of photosensitizer molecules to the ground-state triplet oxygen according to energy transfer theory.[45] In Series-2 corroles, the emission spectra just have a slight blue-shift by the substitutes of the surrounding fluorine atoms, which should have little effect on the efficiency of energy transfer. Therefore, the singlet oxygen quantum yields of Series-2 corroles ultimately depend on the triplet quantum yields. However, for Series-3 corroles, there are relatively large blue-shifts in the emission spectra, which may largely reduce the efficiency of energy transfer. In this case, the singlet oxygen quantum yields mainly depend on the efficiency of energy transfer. This may be exploited to explain the lower singlet oxygen quantum yield observed in the two gallium corroles even though their higher triplet quantum yields with respect to the corresponding free-base corroles.

Finally, our data indicate that the substitutes of the halogen atoms in the surrounding of corrole rings are able to effectively improve the singlet oxygen quantum yield of corroles, and the monohydroxyl corrole bearing iodine (Corrole-I) exhibits the highest singlet oxygen quantum yield among all tested corroles. On the other hand, the incorporation of gallium in the center of corroles can greatly enhance fluorescence quantum yields, the maximum of which was observed for F15-Ga.

CONCLUSION

The luminescent properties, excited-state absorption, and the efficiency of singlet oxygen generation have been investigated in three sets of corroles including monohydroxyl halogen corroles, peripherally fluorine-substituted corroles, and gallium complexes. The experimental data indicate that the heavy atom effects of the substituents and their positions on the photophysical properties of corroles are substantially different. The insertion of gallium into the center of corroles can efficiently enhance fluorescence emission whereas lower the singlet oxygen quantum yields. The monohydroxyl halogenation of corroles can reduce the fluorescence emission but increase the singlet oxygen quantum yield. The efficiency of singlet oxygen generation is determined by not only the triplet state population but also the efficiency of energy transfer from lowest triplet state of a photosensitizer to ground-state oxygen. Our work may be helpful for the further study on the design of corrole derivatives as promising PDT or PDD photosensitizers.

ASSOCIATED CONTENT

Supporting Information

Additional figures. This material is available free of charge via the Internet at http://pubs.acs.org.

AUTHOR INFORMATION

Corresponding Author

*E-mail stswh@mail.sysu.edu.cn; zhlei28@mail.sysu.edu.cn; chhyliu@scut.edu.cn.

Notes

The authors declare no competing financial interest.

ACKNOWLEDGMENTS

This work was financially supported by National Natural Science Foundation of China (Nos. 61178037, 11004256, and 21171057), National Basic Research Program (973 Program) of China under Grant 2013CB922403, and the Open Fund of the State Key Laboratory of optoelectronic Materials and Technologies (Sun Yat-sen University).

REFERENCES

(1) Dougherty, T. J.; Gomer, C. J.; Henderson, B. W.; Kessel, D.; Korbelik, M.; Moan, J.; Peng, Q. *J. Natl. Cancer Inst.* **1998**, *90*, 889−905.
(2) Woodburn, H.; Chang, C. K.; Lee, S.; Henderson, B.; Kessel, D. *Photochem. Photobiol.* **1994**, *60*, 154−159.
(3) Allison, R. R.; Downie, G. H.; Cuenca, R.; Hu, X. H.; Childs, J. C.; Sibata, C. H. *Photodiagn. Photodyn. Ther.* **2004**, *1*, 27−42.
(4) Chang, C. K.; Kong, P. W.; Liu, H. Y.; Yeung, L. L.; Koon, H. K.; Mak, N. K. *Proc. SPIE* **2006**, *6139*, 15−1−11.
(5) Gorman, A.; Killoran, J.; O'Shea, C.; Kenna, T.; Gallagher, W. M.; O'Shea, D. F. *J. Am. Chem. Soc.* **2004**, *126*, 10619−10631.
(6) Hirakawa, K.; Kawanishi, S.; Hirano, T.; Segawa, H. *J. Photochem. Photobiol., B* **2007**, *87*, 209−217.
(7) Kořínek, M.; Dědic, R.; Molnár, A.; Hála, J. *J. Fluoresc.* **2006**, *16*, 355−359.
(8) Azenha, E. G.; Serra, A. C.; Pineiro, M.; Pereira, M. M.; Seixas de Melo, J.; Arnaut, L. G.; Formosinho, S. J.; Rocha Gonsalves, A. M. d'A. *Chem. Phys.* **2002**, *280*, 177−190.
(9) Shi, L.; Liu, H. Y.; Shen, H.; Hu, J.; Zhang, G. L.; Wang, H.; Ji, L. N.; Chang, C. K.; Jiang, H. F. *J. Porphyrins Phthalocyanines* **2009**, *13*, 1221−1226.
(10) Vestfrid, J.; Botoshansky, M.; Palmer, J. H.; Durrell, A. C.; Gray, H. B.; Gross, Z. *J. Am. Chem. Soc.* **2011**, *133*, 12899−12901.
(11) Prodi, A.; Kleverlaan, C. J.; Indelli, M. T.; Scandola, F. *Inorg. Chem.* **2001**, *40*, 3498−3504.
(12) (a) Aviv-Harel, I.; Gross, Z. *Coord. Chem. Rev.* **2011**, *255*, 717−736. (b) Aviv-Harel, I.; Gross, Z. *Chem.—Eur. J.* **2009**, *15*, 8382−8394.
(13) Lai, W. Z.; Cao, R.; Gong, G.; Shaik, S.; Yao, J. N.; Chen, H. *J. Phys. Chem. Lett.* **2012**, *3*, 2315−2319.
(14) (a) Ding, T.; Aleman, E. A.; Modarelli, D. A.; Ziegler, C. J. *J. Phys. Chem. A* **2005**, *109*, 7411−7417. (b) Ventura, B.; Degli Esposti, A.; Koszarna, B.; Gryko, D. T.; Flamigni, L. *New J. Chem.* **2005**, *29*, 1559−1566.
(15) Liu, X.; Mahammed, A.; Tripathy, U.; Gross, Z.; Steer, R. P. *Chem. Phys. Lett.* **2008**, *459*, 113−118.
(16) Kowalska, D.; Liu, X.; Tripathy, U.; Mahammed, A.; Gross, Z.; Hirayama, S.; Steer, P. *Inorg. Chem.* **2009**, *48*, 2670−2676.
(17) Bendix, J.; Dmochowsky, I. J.; Gary, H. B.; Mahammed, A.; Simkhovich, L.; Gross, Z. *Angew. Chem., Int. Ed.* **2000**, *39*, 4048−4051.
(18) Aviezer, D.; Cotton, S.; David, M.; Segev, A.; Khaselev, N.; Galili, N.; Gross, Z.; Yayon, A. *Cancer Res.* **2000**, *60*, 2973−2980.
(19) Lim, P.; Mahammed, A.; Okun, Z.; Saltsman, I.; Gross, Z.; Gary, H. B.; Termini, J. *Chem. Res. Toxicol.* **2012**, *25*, 400−409.
(20) Hwang, J. Y.; Lubow, J.; Chu, D.; Ma, J.; Agadjanian, H.; Sims, J.; Gray, H. B.; Gross, Z.; Farkas, D. L.; Medina-Kauwe, L. K. *Mol. Pharmaceutics* **2011**, *8*, 2233−2243.
(21) Hwang, J. Y.; Gross, Z.; Gray, H. B.; Medina-Kauwe, L. K.; Farkas, D. L. *J. Biomed. Opt.* **2011**, *16*, 066007.
(22) Hwang, J. Y.; Lubow, D. J.; Sims, J. D.; Gray, H. B.; Mahammed, A.; Gross, Z.; Medina-Kauwe, L. K.; Farkas, D. L. *J. Biomed. Opt.* **2012**, *17*, 015003.

(23) Agadjanian, H.; Ma, J.; Rentsendorj, A.; Valluripalli, V.; Hwang, J. Y.; Mahammed, A.; Farkas, D. L.; Gray, H. B.; Gross, Z.; Medina-Kauwe, L. K. *Proc. Natl. Acad. Sci. U. S. A.* **2009**, *106*, 6105−6110.
(24) Gryko, D. T.; Koszarna, B. *Org. Biomol. Chem.* **2003**, *1*, 350−357.
(25) Gross, Z.; Galili, N.; Saltsman, I. *Angew. Chem., Int. Ed.* **1999**, *38*, 1427−1429.
(26) Nardis, S.; Monti, D.; Paolesse, R. *Mini-Rev. Org. Chem.* **2005**, *2*, 355−374.
(27) Shimo, N.; Nakashima, N.; Yoshihara, K. *Laser Flash Photolysis Benzene* **1983**, *56*, 389−399.
(28) (a) Staveren, D. R.; Albada, G. A.; Haasnoot, J. G.; Kooijman, H.; Lanfredi, A. M. M.; Nieuwenhuizen, P. J.; Spek, A. L.; Ugozzoli, F.; Weyhermuller, T.; Reedijk, J. *Inorg. Chim. Acta* **2001**, *315*, 163−171. (b) Dong, S. S.; Nielsen, R. J.; Palmer, J. H.; Gary, H. B.; Gross, Z.; Dasgupta, S.; Goddard, W. A., III *Inorg. Chem.* **2011**, *50*, 764−770.
(29) Liu, B.; Yu, W. L.; Lai, Y. H.; Huang, W. *Chem. Mater.* **2001**, *13*, 1984−1991.
(30) Santos, C. I. M.; Oliveira, E.; Barata, J. F. B.; Faustino, M. A. A. F.; Cavaleiro, J. A. S.; Neves, M.; Grac, A. P. M. S.; Lodeiro, C. *J. Mater. Chem.* **2012**, *22*, 13811−13819.
(31) Ghosh, A.; Wondimagegn, T.; Parusel, A. B. J. *J. Am. Chem. Soc.* **2000**, *122*, 5100−5104.
(32) Do Rough, G. D.; Miller, J. R.; Huennekens, F. *Spectra of Metallo-Derivatives of αβγ-Tetraphenylporphine* **1951**, *73*, 4315−4320.
(33) Karweik, D. H.; Winograd, N. *Inorg. Chem.* **1956**, *15*, 2337−2342.
(34) Mahammed, A.; Gross, Z. *J. Inorg. Biochem.* **2002**, *88*, 305−309.
(35) Zhang, X. F.; Huang, J.; Xi, Q.; Wang, Y. *Aust. J. Chem.* **2010**, *63*, 1471−1476.
(36) Pelegrino, A. C.; Carolina, M. M.; Gotardo.; Simioni, A. R.; Assis, M. D.; Tedesco, A. C. *Photochem. Photobiol.* **2005**, *81*, 771−776.
(37) Wilkinson, F.; Helman, W. P.; Ross, A. B. *J. Phys. Chem. Ref. Data* **1993**, *22*, 113−262.
(38) Tanielian, C.; Wolff, C. *J. Phys. Chem.* **1995**, *99*, 9825−9830.
(39) (a) Koziar, J. C.; Cowan, D. O. *Acc. Chem. Res.* **1978**, *11*, 334−341. (b) Nifiatis, F.; Athas, J. C.; Gunaratne, K. D. D.; Gurung, Y.; Monette, K. M.; Shivokevich, P. J. *Open Spectrosc. J.* **2011**, *5*, 1−12.
(40) Ha, J. H.; Jung, G. Y.; Kim, M. S.; Lee, Y. H.; Shin, K.; Kim, Y. R. *Bull. Korean Chem. Soc.* **2001**, *22*, 63−67.
(41) Murov, S. L.; Carmichael, I.; Hug, G. L. *Handbook of Photochemistry*; Marcel Dekker, Inc.: New York, 1993.
(42) Mathai, S.; Smith, T. A.; Ghiggino, K. P. *Photochem. Photobiol. Sci.* **2007**, *6*, 995−1002.
(43) (a) Grossweiner, L. I. Singlet oxygen: generation and properties, http://www.photobiology.com/education/len2. (b) Abdel-Shafi, A. A.; Worrall, D. R. *J. Photochem. Photobiol. A: Chem.* **2005**, *172*, 170−179.
(44) Rejo Jeice, A.; Navaneethakrishanan, K. *Braz. J. Phys.* **2009**, *39*, 526−530.
(45) (a) Forater, T. H. *Radiat. Res. Suppl.* **1960**, *2*, 326−339. (b) Speiser, S. *Chem. Rev.* **1996**, *96*, 1953−1976.